AFRL-RX-WP-JA-2015-0068

PLASMONIC RESONANCES IN SELF-ASSEMBLED REDUCED SYMMETRY GOLD NANOROD STRUCTURES (POSTPRINT)

Sushmita Biswas, Jinsong Duan, Dhriti Nepal, Ruth Pachter, and Richard Vaia
AFRL/RXA

MAY 2013
Interim Report

AIR FORCE RESEARCH LABORATORY
MATERIALS AND MANUFACTURING DIRECTORATE
WRIGHT-PATTERSON AIR FORCE BASE, OH 45433-7750
AIR FORCE MATERIEL COMMAND
UNITED STATES AIR FORCE

NOTICE AND SIGNATURE PAGE

Using Government drawings, specifications, or other data included in this document for any purpose other than Government procurement does not in any way obligate the U.S. Government. The fact that the Government formulated or supplied the drawings, specifications, or other data does not license the holder or any other person or corporation; or convey any rights or permission to manufacture, use, or sell any patented invention that may relate to them.

This report was cleared for public release by the USAF 88th Air Base Wing (88 ABW) Public Affairs Office (PAO) and is available to the general public, including foreign nationals.

Copies may be obtained from the Defense Technical Information Center (DTIC) (http://www.dtic.mil).

AFRL-RX-WP-JA-2015-0068 HAS BEEN REVIEWED AND IS APPROVED FOR PUBLICATION IN ACCORDANCE WITH ASSIGNED DISTRIBUTION STATEMENT.

//Signature//	//Signature//
RICHARD A. VAIA	KAREN R. OLSON, Deputy Chief
Functional Materials Division	Functional Materials Division
Materials and Manufacturing Directorate	Materials and Manufacturing Directorate

This report is published in the interest of scientific and technical information exchange, and its publication does not constitute the Government's approval or disapproval of its ideas or findings.

REPORT DOCUMENTATION PAGE

Form Approved
OMB No. 074-0188

1. REPORT DATE (DD-MM-YYYY)	2. REPORT TYPE	3. DATES COVERED *(From – To)*
May 2013	Interim	05 November 2009 – 09 April 2013

4. TITLE AND SUBTITLE
PLASMONIC RESONANCES IN SELF-ASSEMBLED REDUCED SYMMETRY GOLD NANOROD STRUCTURES (POSTPRINT)

5a. CONTRACT NUMBER
In-House

5b. GRANT NUMBER

5c. PROGRAM ELEMENT NUMBER
62102F

6. AUTHOR(S)
(see back)

5d. PROJECT NUMBER
4347

5e. TASK NUMBER

5f. WORK UNIT NUMBER
X03Z

7. PERFORMING ORGANIZATION NAME(S) AND ADDRESS(ES)
(see back)

8. PERFORMING ORGANIZATION REPORT NUMBER

9. SPONSORING / MONITORING AGENCY NAME(S) AND ADDRESS(ES)
Air Force Research Laboratory
Materials and Manufacturing Directorate
Wright Patterson Air Force Base, OH 45433-7750
Air Force Materiel Command
United States Air Force

10. SPONSOR/MONITOR'S ACRONYM(S)
AFRL/RXA

11. SPONSOR/MONITOR'S REPORT NUMBER(S)
AFRL-RX-WP-JA-2015-0068

12. DISTRIBUTION / AVAILABILITY STATEMENT
Distribution A. Approved for public release; distribution unlimited. This report contains color.

13. SUPPLEMENTARY NOTES
PA Case Number: 88ABW-2013-2338, Clearance Date: 15 May 2013. Journal article published in P Nano Lett. 2013, 13, 2220−2225. © 2013 American Chemical Society. The U.S. Government is joint author of the work and has the right to use, modify, reproduce, release, perform, display or disclose the work. The final publication is available at dx.doi.org/10.1021/nl4007358.

14. ABSTRACT
Self-assembled plasmonic Dolmen structures consisting of small gold nanorods (length = 50 nm and diameter = 20 nm) with a few nanometer gaps are observed to show coherent effects of super-radiance and characteristics of Fano resonance due to the significantly reduced symmetry of the structure. Relative to previous larger structures from top-down electron-beam lithography, the single crystallinity and atomically smooth surfaces of these self-assembled plasmonic structures result in 50% narrower resonances, and the small gaps with associated strong coupling enable observation of multiple dark and bright modes. By tilting the cap monomer with respect to the base dimer an order of magnitude increase in E-field enhancement at the Fano dip is obtained. In addition, a spectrally broad mode is observed indicating the strong impact of the geometry of the structure on the nature of coupled modes. The highly localized electric near-fields in the gaps will enable strong light matter interactions and the narrow resonances will be useful for improved figure of merits in inexpensive chemical and biosensing.

15. SUBJECT TERMS
surface plasmons, dark modes, Dolmen, Fano resonances, gold nanorods

16. SECURITY CLASSIFICATION OF:			17. LIMITATION OF ABSTRACT	18. NUMBER OF PAGES	19a. NAME OF RESPONSIBLE PERSON *(Monitor)*
a. REPORT	b. ABSTRACT	c. THIS PAGE			Richard A. Vaia
Unclassified	Unclassified	Unclassified	SAR	10	19b. TELEPHONE NUBER *(include area code)* (937) 255-9209

REPORT DOCUMENTATION PAGE Cont'd

6. AUTHOR(S)

Sushmita Biswas, Jinsong Duan, Dhriti Nepal, Ruth Pachter, and Richard Vaia - Materials and Manufacturing Directorate, Air Force Research Laboratory, Functional Materials Division

7. PERFORMING ORGANIZATION NAME(S) AND ADDRESS(ES)

AFRL/RXA
Air Force Research Laboratory
Materials and Manufacturing Directorate
Wright-Patterson Air Force Base, OH 45433-7750

NANO LETTERS

Letter

pubs.acs.org/NanoLett

Plasmonic Resonances in Self-Assembled Reduced Symmetry Gold Nanorod Structures

Sushmita Biswas, Jinsong Duan, Dhriti Nepal, Ruth Pachter, and Richard Vaia*

Air Force Research Laboratory, 2941 Hobson Way, Wright Patterson Air Force Base, Ohio 45433, United States

Supporting Information

ABSTRACT: Self-assembled plasmonic Dolmen structures consisting of small gold nanorods (length = 50 nm and diameter = 20 nm) with a few nanometer gaps are observed to show coherent effects of super-radiance and characteristics of Fano resonance due to the significantly reduced symmetry of the structure. Relative to previous larger structures from top-down electron-beam lithography, the single crystallinity and atomically smooth surfaces of these self-assembled plasmonic structures result in 50% narrower resonances, and the small gaps with associated strong coupling enable observation of multiple dark and bright modes. By tilting the cap monomer with respect to the base dimer an order of magnitude increase in E-field enhancement at the Fano dip is obtained. In addition, a spectrally broad mode is observed indicating the strong impact of the geometry of the structure on the nature of coupled modes. The highly localized electric near-fields in the gaps will enable strong light matter interactions and the narrow resonances will be useful for improved figure of merits in inexpensive chemical and biosensing.

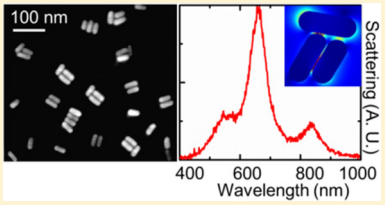

KEYWORDS: *Surface plasmons, dark modes, Dolmen, Fano resonances, gold nanorods*

Engineered plasmonic metamaterials are of significant interest for a broad swath of photonic technologies, ranging from ultrasensitive chemical and biosensing,[1−3] to nanolasing,[4] spectroscopy,[5,6] photovoltaics,[7] and photodetection[8] due to the ability to confine light below the diffraction limit and control light-matter interactions.[9−11] Subradiant or dark modes in plasmonic systems are especially interesting due to their inherent small line-width, high quality factor (Q) and reduced radiative losses, which have special significance for nanolasing, waveguiding, and sensing.[12−15] For example, Yanik and co-workers utilized dark modes to demonstrate a record figure of merit for biomolecule detection that far exceeded theoretical limits of surface plasmon resonance sensors (considered the gold-standard technology).[16] These modes however are difficult to access since they couple weakly to the incident light due to their near-zero dipole moment. Overall, the continual maturation of plasmonic metamaterials necessitates control of radiative loss pathways in these structures. Losses lower the quality factor of a resonance, where high Q resonance is desirable for higher near-field enhancement and stronger light matter interactions.[9,12,17] Whereas intrinsic or nonradiative losses are material dependent, radiative losses can be minimized by material engineering by exploiting dark modes and Fano resonances.[9]

One of the simplest systems where symmetry breaking allows the manifestation of the dark modes is a nanorod (NR) dimer.[1,2,13,18−20] Methods to reveal dark modes in this system include creating offsets between the pair,[21,22] heterodimer configuration[23−25] and offset illumination schemes.[26] An alternative approach is to break the symmetry by bringing in a third NR to one end, the so-called "Dolmen" structure.[1,27,28] This structure has shown Fano resonances and is predicted to exhibit plasmonic electromagnetically induced transparency (EIT).[28] Limits on resolution and surface roughness (large units >100 nm in length and 10s of nm in gaps fabricated by top-down lithography) however broadened the resonances of previously investigated Dolmens.[1,27] This restricted the sharpness of the dips minimizing the EIT and the extent of local field enhancement. Sharper resonances necessitate atomically smooth surfaces and normalized gap distances, $s/l < 0.06$, where s is the gap distance and l is the length of the nanoparticles.[21,26] Such a small gap (0.5−3 nm) increases coulomb attractive forces between induced charges resulting in a stronger near-field enhancement.[26] Also the dipole−multipole interactions mediated by such gaps result in a multitude of confining and radiative modes that are difficult to observe in larger counterparts.[21,26,29] Finally, these small gaps provide ultrasmall mode volumes for field confinement, providing opportunities for enormous Purcell enhancement of spontaneous emission of a fluorophore compared to that achieved by a single NR.[26] In general, these desirable geometric features are commensurate with bottom-up assembly of single crystal NRs if concepts can be established to break assembly symmetry.

In this paper, we demonstrate multiple radiative (bright) and confining (dark or subradiant) modes in Dolmen structures (with 0.5−2.0 nm gap sizes) created by bottom-up assembly of chemically synthesized colloidal gold NRs (length = 50 nm; diameter = 20 nm) stabilized with cetyl-trimethyl-ammonium-bromid (CTAB) bilayer.[30] Using these single crystalline monomers and small surfactant-defined gaps of 0.5−2.0 nm,

Received: February 26, 2013
Revised: April 9, 2013
Published: April 22, 2013

the radiative losses are substantially reduced as observed from the sharpness of the assembled Dolmen's resonances. The amount of energy coupling to the dark mode depends on the relative orientation of the cap NR to the base dimer, providing a factor of 3 higher electric field enhancement in a strongly coupled (SC) system (slightly tilted Dolmen) as compared to a weakly coupled (WC) one (distorted Dolmen). Characteristics of Fano resonance are observed in both the systems. An order of magnitude increase in E-field enhancement at the Fano dip is obtained in the WC Dolmen compared to the SC system due to its geometry and significantly reduced radiative nature of the dark mode. Finally, a spectrally broad mode similar to a super-radiant mode is observed depending on the relative orientation of the cap monomer. These self-assembled Dolmens demonstrate a route to improving the quality of the plasmonic structure and will be of significant interest for future design of nanophotonic devices including single photon sources, nano-lasers, and displays.

The Dolmen cavities used in this study are synthesized by assembly of chemically synthesized AuNRs,[30] the details of which are provided in the Supporting Information, Section S.I.I. The AuNRs are separated from each other in the assembly with a cetyl-trimethyl-ammoniumbromide (CTAB) bilayer (~2.4 nm thick).[26,30,31] The advantages that this method offers over other top-down methods are controlled variation in gap sizes through the use of various surfactants, and single crystal monomers[32] with atomically smooth surfaces. The latter reduces the radiative scattering arising from rough surfaces. The resulting nanostructures have a distribution in the position and alignment of the cap NR with respect to the base dimer, as shown in the scanning electron microscope (SEM) image in Figure 1a. To demonstrate the spectral quality and potential for tunability inherent in this bottom-up assembly process, we perform a detailed investigation of two types of Dolmens, a SC and a WC system determined by different angles of tilt between the long axes of the cap AuNR and the base dimer. A general schematic of the tilted Dolmens is depicted in Figure 1c where α is the angle of tilt. Single particle scattering spectrum was collected with an Olympus BX41 optical dark-field microscope [Figure 1d, equipped with a halogen white light source, a Thorlabs broadband (0.5−1.4 μm) thin film polarizer, a dark-field oil immersion condenser (N.A. 1.4) and an objective lens (N.A. 0.7−1.4)-CytoViva]. The scattering spectra are normalized with the optical response of the experimental setup. Single particle measurements are correlated with SEM to provide structural parameters,[33] as shown in Figure 1b. Finite difference time domain (FDTD) modeling and analytical formulation of Maier[34] et al. on plasmonic interferences provided estimations of the scattering spectra, charge distributions and insight to mode coupling.

The structure and scattering properties of a tilted Dolmen with $\alpha = 107°$ are presented in Figure 2. The SEM image of the structure is shown in Figure 2a and the dimensions are provided in the figure caption. We refer to this structure as a SC Dolmen for reasons that will follow. This nanostructure consists of two subunits: a heterodimer with AuNRs in the base separated by 0.5−2.0 nm and a cap NR separated by 0.5−2.0 nm. The dimensions are based on SEM measurements, corroborated with statistical TEM measurements on similar structures and are in good agreement with recent reports.[26] Note that more precise measurements of a particular nanostructure require high resolution SEM imaging, which

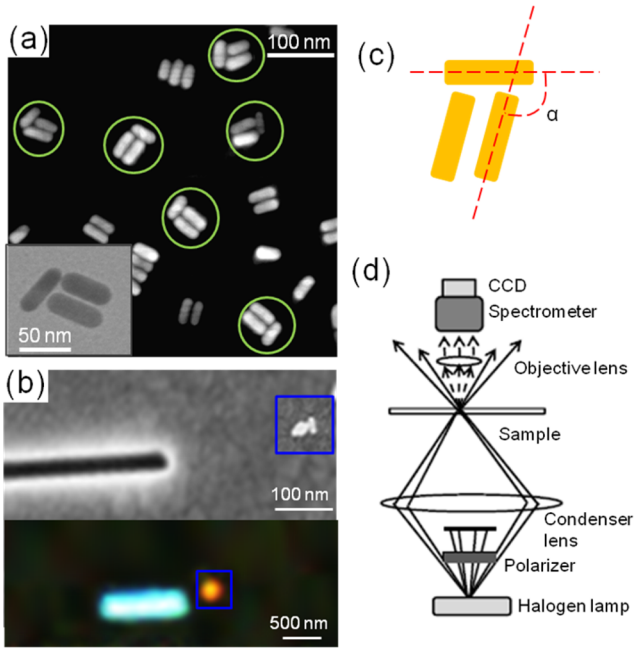

Figure 1. Characterization of Dolmens. (a) SEM image of Dolmens on silicon substrate synthesized chemically from AuNRs (l = 50 ± 2 nm, d = 20 ± 2 nm, and gap distances of 0.5−2 ± 0.5 nm). (b) SEM-correlated dark-field microscopy; bottom inset shows dark-field optical image of the area shown in SEM image. (c) General schematic of Dolmen conveying the tilt angle α between monomer cap and dimer base. (d) Schematic of polarized dark-field optical scattering microscope.

damages features of nanoparticles, reducing the certainty of structural measurements and changes its optical response.[31]

For the SC Dolmen, the scattering spectrum polarized parallel to cap (Figure 2h, solid line) shows three peaks around 570 (PI), 650 (PII), and 850 (PIII) and two dips at 600 nm (DI) and 750 nm (DII). The dip DII displays a prominent asymmetric line shape for this polarization. The asymmetry is indicative of a dispersive coupling and characteristic of a Fano resonance. The asymmetry disappears at the near-orthogonal polarization (Figure 2g). Overall, the resonances are ~50% narrower than previously observed.[1,27] The evolution of the spectra as incident polarization direction is rotated is presented in Figure 2j. Corresponding classical electromagnetic FDTD simulations of the scattering are shown in Figure 2h (dashed line). The AuNRs in the assembly are modeled as cylinders with hemispherical caps. A gap distance was adjusted to 0.5 nm within the experimentally measured range to reach a good agreement with measured results. The refractive index of the top and side medium is chosen as 1 and the glass medium underneath is 1.5. The calculated spectra with two different mesh sizes (0.5 and 0.2 nm) reproduce the measured spectral peaks, and indicate near-convergence of the far-fields (Supporting Information Figure S1). The presence of a substrate does not alter the features qualitatively beyond a red shift induced by refractive index (Supporting Information Figure S4). The small shoulder appearing at 700 nm in the calculated spectra (blue dashed line) from polarization parallel to cap NR is not investigated, as it disappears at finer mesh sizes (Supporting Information Figure S1) and is not present in the experimental spectrum. The discussions around charge densities and electric field enhancements are for 0.5 nm mesh size (corresponding results at 0.2 nm mesh are provided in

dx.doi.org/10.1021/nl4007358 | Nano Lett. 2013, 13, 2220−2225

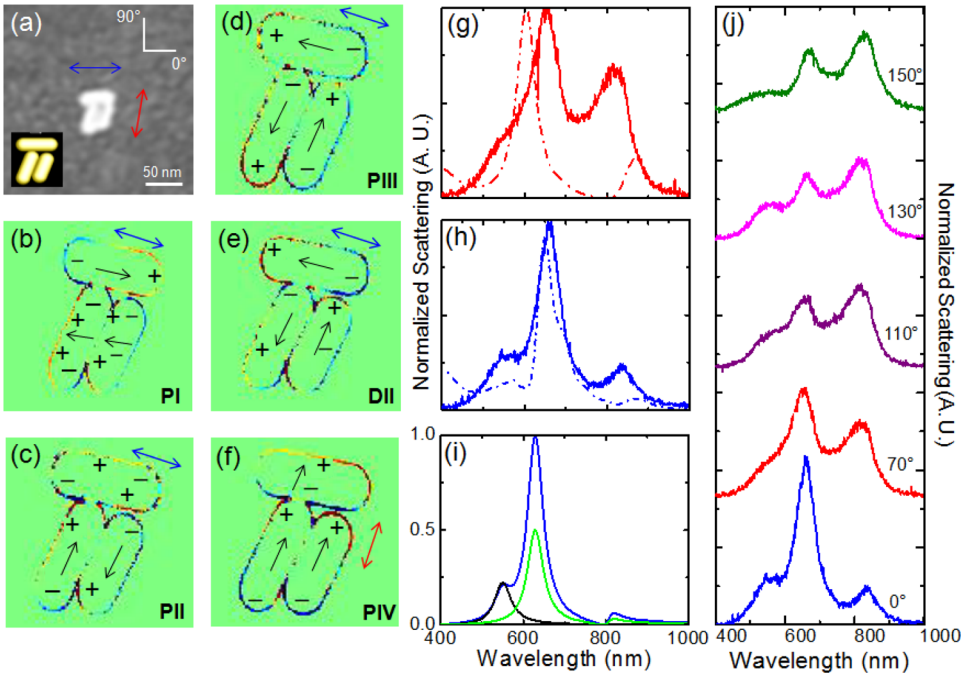

Figure 2. Strongly coupled (SC) Dolmen. (a) SEM image of SC Dolmen with dimensions: left AuNR, length l = 52 nm, diameter d = 20 nm; right AuNR, l = 56 nm, d = 20 nm; cap AuNR, l = 56 nm, d = 22 nm, gap within dimer base ~0.5−2.0 nm, between cap and dimer base ~0.5−2.0 nm; diameters 20.0 nm, tilt angle α = 107°. Two major polarization directions parallel to the long axis of cap and dimer base are depicted by blue and red arrows respectively and a schematic of the structure is provided in inset. (b−f) FDTD charge density profiles at peaks PI, PII, PIII and dip DII for blue polarization direction and PIV for red polarization direction. (g,h) Polarized dark-field (solid) and FDTD modeled (dashed) scattering spectra for red and blue polarization directions respectively. (i) Analytical scattering profile for the blue polarization direction where blue curve is the sum of the scattering contributions from (I) interaction between cap dipolar mode $\lambda_{p\text{-}cap}$ = 630 nm and bonding dark mode in the dimer $\lambda_{d\text{-}dimer}$ = 800 nm with Γ_p = 0.2, v = 2.0*g_0, w = 1.1*g_0 (green) where g_0 = 0.2 and (II) a Lorentzian dipolar bright mode in dimer $\lambda_{p\text{-}dimer}$ = 550 nm (black). (j) Evolution of the dark-field scattering spectra at different polarization directions (0−150°).

Supporting Information Figure S2 and S3). The small gap size limits the number of cells spanning the gap to 1−2, restricting the convergence of the near-fields.[26,35] Finer Cartesian grids (<0.1 nm) are limited by computational resources and inadequate description of the entire gap region due to the distorted nature of the structure. Hence the reported field enhancement reflect lower bounds of the actual enhancement at the metal surface. The relative ratio however is consistent for different meshes and provides a means to discuss impact of structure on enhancement. In general, the agreement between experimental and calculated spectra is good and within previously reported uncertainties.[27] Note that the plasmonic response of dimers with subnanometer separation distances presents an experimental as well as theoretical challenge requiring both quantum mechanical and classical electromagnetic modeling.[36,37] Herein though, classical electromagnetic modeling provided good agreement with respect to the fidelity of the experimental results, so the addition of the quantum corrected model for small interacting plasmonic systems[37] is unwarranted.

The FDTD charge distribution plots depicted in Figure 2b−f, reveal different plasmon modes of the SC Dolmen. For polarization parallel to cap, the peak PI corresponds to transverse dipoles aligned in the dimer and an opposite dipole in the cap. Peak PII shows a bonding mode in the dimer with dipoles aligned in opposite directions, and mixed dipolar and quadrupolar mode in the cap. The near-field of the cap couples to the bonding mode in the dimer which in turn couples to the quadrupolar mode in the cap. Hence we refer to this as a SC system. Peak PIII corresponds to the bonding mode in the dimer, and a dipolar mode in the cap. Note that this mode has some similarity to a conductive plasmon in a dimer, which would arise due to physical overlap of the AuNRs.[31] Such a mode is unlikely to occur in these Dolmens however due to the presence of an organic CTAB bilayer (~2.4 nm thick) between the dimer.[26,30,31] The nature of the modes at DII shows that the near-field of the cap couples to a bonding mode in the dimer creating the Fano line shape. The dip DI corresponds to an antibonding dipolar mode in the dimer and a dipolar mode in the cap (Supporting Information Figure S4b). In contrast, when the polarization is rotated parallel to the dimer long axis (70°, Figure 2g), the two resonance peaks at 610 nm (PIV) and 870 nm (PV) correspond to the antibonding dipolar mode (Figure 2f) and a bonding mode (not shown) similar to PIII. From the nature of the charge distributions and the location of the electric field hotspots in Figure 3 and Figure S6 (Supporting Information), we assign PI, PIV to be radiative modes or bright modes and, PII, PIII to be confining modes or dark modes. Note that two additional Dolmens with comparable structure and gaps have similar spectral features in unpolarized light, as shown in Figure S5 (Supporting Information).

The spatial average values (over multiple points discarding the highest intensity single point) of electric field intensities ($|E|^2$) occurring at the peaks and dips of the SC Dolmen when excited parallel to the cap are listed in Table 1. The value for a single AuNR is included for comparison. The largest (average) electric field enhancement for the SC Dolmen is ~2800 (1700) at PII and localized within the gaps of the dimer (Figure 3a). At the lower energy dip DII, this maximum (average) enhance-

dx.doi.org/10.1021/nl4007358 | Nano Lett. 2013, 13, 2220−2225

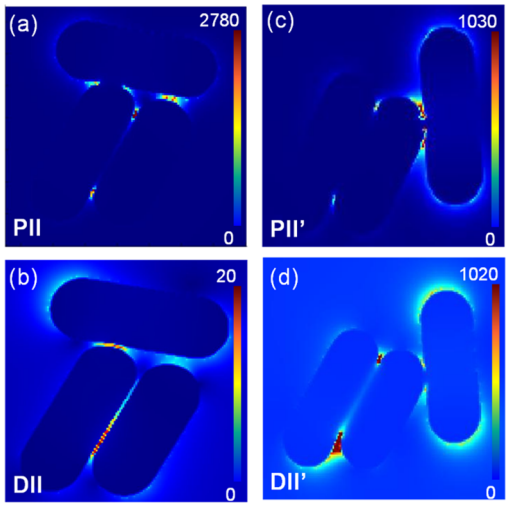

Figure 3. Electric near-field profiles showing the hotspots of SC and WC Dolmens at different spectral locations. (a) PII, (b) DII, (c) PII′, and (d) DII′. Color scale has been adjusted for better depiction of the field hot spots.

Table 1. Average E-Field Intensities ($|E|^2$) at the Peaks and Dips for SC and WC Dolmens at Polarization Parallel to the Cap NR

	PI	DI	PII	DII	PIII
SC Dolmen	700	60	1700	15	1200
WC Dolmen	300	250	515	450	900
single AuNR (630 nm)	120				

ment is much lower, 20 (15). Although DII displays a line shape characteristic of a Fano resonance and field enhancement within the gap of the dimer (Figure 3b), the local E-fields are not as enhanced as for the dark mode at peak PII. The hot spots of the electric near-field at PII and DII are localized within the gap of the dimer. The associated ultrasmall mode volume could provide opportunities for large Purcell enhancement of spontaneous emission of a fluorophore placed in the gap.

The analytical approach of plasmonic interferences of Maier et al.[34] provides additional insight on the coherent interactions taking place in these perturbed Dolmens. The scattering intensity profile resulting from the interference of two spectrally close states is given by

$$F'(E) = g^2 \mathcal{L}^* F(E) \quad (1)$$

here E is the energy of the incident photon, g is the probability of direct excitation of dipolar bright state, $\mathcal{L}(E)$ is the Lorenztian line shape of the bright state and $F(E)$ is Fano profile function described in the Supporting Information S.I. III.

Here the Dolmen can be deconstructed into two subunits (cap NR and base dimer) and the scattering profile can be estimated from the interference of the resonances from these subunits. Approximate values of resonances of the subunits are obtained from FDTD calculations, where the wavelengths of the bright dipolar mode of the cap NR is λ_{p-cap} = 630 nm (longitudinal polarization) and the bright dipolar and dark bonding modes of the base dimer are $\lambda_{p-dimer}$ = 550 nm and $\lambda_{d-dimer}$ = 800 nm (parallel polarization to short axis of dimer) (Supporting Information Figure S7). The resulting scattering profile for polarization parallel to cap (blue line Figure 2i) shows a close agreement with the experimental data (Figure 2h) and is the outcome of a Fano interaction between λ_{p-cap} and $\lambda_{d-dimer}$ linearly superposed with the Lorentzian function of $\lambda_{d-dimer}$. As expected the coupling parameters described in Figure 2i and associated caption, show that the Fano interaction is strong with a coupling parameter (v = 2.0*g_0 and g_0 = 0.2 where v is defined in the Supporting Information S.I. III as the probability of the interaction between the dark and bright states) and there is significant probability of direct excitation of the dark state at $\lambda_{d-dimer}$ (w = 1.1*g_0) indicating its radiative coupling to the far-field. Although the relative intensities of the peaks are different from the experimental and modeled results, this method gives qualitative insight to the nature of interactions taking place in such a complex plasmonic system by revealing the relation of the modes to the subunits that comprise the structure. The asymmetric line shape at DII is also revealed in this analytical calculation. The poor spectral overlap between dark and bright modes, the broadness of the dark mode as well as significantly high radiative nature of the dark mode are consistent with the poor E-field enhancement at the Fano resonance dip DII (Table 1).

Following from the earlier discussion, the symmetry of the structure is critical for coupling of incident light to different bright and dark plasmonic resonances. Hence a distorted Dolmen with different relative orientation of the cap NR to the base dimer is investigated (Figure 4a). Rotation of the cap relative to the base dimer (decreasing α) will decrease the coupling between these subunits. Figure 4 summarizes the scattering spectra and associated modeling for such a weakly coupled (WC) Dolmen (α = 60°). When the incident light is parallel to the cap, the scattering spectrum (solid line, Figure 4h) consists of three peaks around 570 nm (PI′), 640 nm (PII′), and 780 nm (PIII′) and two dips at 600 nm (DI′) and 760 nm (DII′). These modes are observed in the calculated spectra (dashed line, Figure 4h). The charge distributions depicted in Figure 4b−f show that PI′ and DI′ (Supporting Information Figure S4c) reflect a dipolar antibonding mode in the dimer coupled to a higher order mode in the cap NR. PII′ shows a bonding mode in the dimer and dipolar mode in the cap. Dip DII′ results from a bonding mode in the dimer coupled to a dipolar mode in the cap NR with a strong contribution from the cap AuNR (a mixed higher order mode can be observed in the right NR in the dimer). Hence even in this highly distorted Dolmen, these two dips have characteristics of a Fano resonance. Overall, the cap couples to the longitudinal antibonding and bonding mode of the dimer base in contrast to the SC Dolmen where the cap couples to the transverse dipolar bonding and longitudinal dipolar bonding mode of the dimer base. Further rotation of the polarization to 20° with respect to laboratory frame of reference causes the appearance of DI′ in the spectrum followed by DII′ at 110°. When the polarization is rotated to 0° (red arrow), a broad resonance peaked at 570 nm (PIV′) with 200 nm full width half-maximum (fwhm) is observed (as opposed to fwhm of 75 nm for single NRs[33] shown in Supporting Information Figure S8). The charge distribution plot shows that the dipoles are aligned in the same direction causing a blue-shifted repulsive antibonding mode compared to that of a single AuNR (resonance peak 630 nm, Supporting Information Figure S7). The resulting antibonding mode consists of dipolar charge oscillations in phase resulting in a super-radiant mode. The broadness in this mode arises due to strong radiative damping.

dx.doi.org/10.1021/nl4007358 | Nano Lett. 2013, 13, 2220−2225

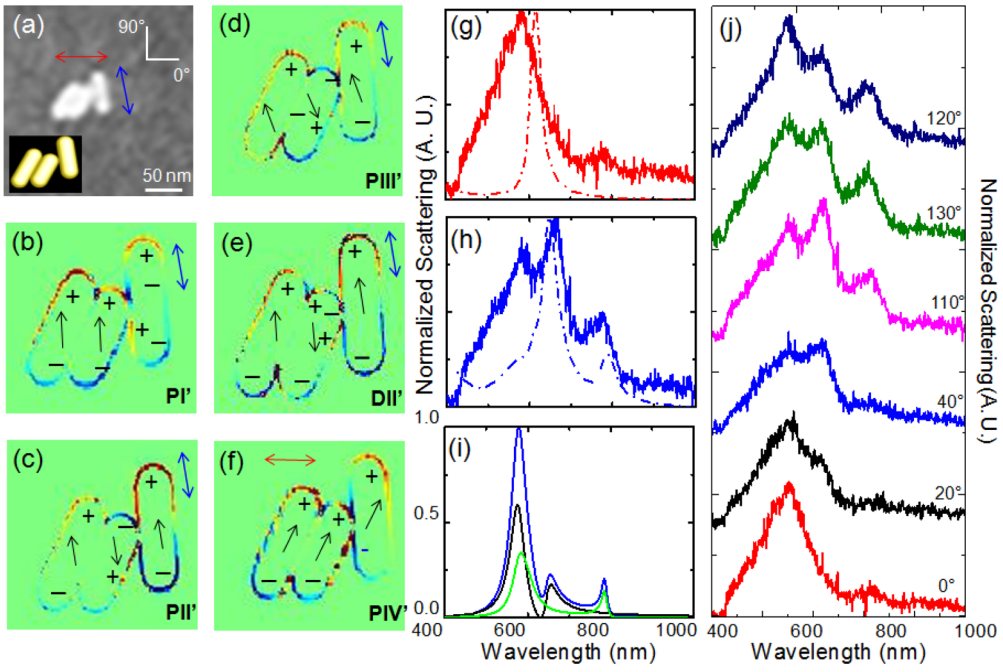

Figure 4. Weakly coupled (WC) Dolmen. (a) SEM image of WC Dolmen with dimensions: left AuNR, length l = 50 nm, diameter d = 18 nm; right AuNR, l = 44 nm, d = 18 nm; cap AuNR, l = 49 nm, d = 17 nm; gap within dimer base ~0.5−2.0 nm; between cap and dimer base ~0.5−2.0 nm; tilt angle α = 60°. Two major polarization directions parallel to the long axis of cap and approximately parallel to the short axis of dimer base in the laboratory frame of reference are depicted by blue and red arrows respectively and a schematic of the structure is provided in inset. (b−f) FDTD charge density profiles at peaks PI′, PII′, PIII′, and dip DII′ for blue polarization direction and PIV′ for red polarization direction. (g,h) Polarized dark-field (solid) and FDTD modeled (dashed) scattering spectra for red and blue polarization directions. (i) Analytical scattering profile for the blue polarization direction where blue curve is the sum of the scattering contributions from interaction between (I) the dipolar mode in the dimer $\lambda'_{\text{p-dimer}}$ = 600 nm and a higher order dark mode in the cap $\lambda'_{\text{d-cap}}$ = 620 nm (black) where Γ_p = 0.25, $v = g_0$, $w = 0.35*g_0$ and (II) the dipolar mode in the cap $\lambda'_{\text{p-cap}}$ = 630 and a bonding mode in the dimer $\lambda'_{\text{d-dimer}}$ = 760 nm (green) where Γ_p = 0.25, $v_1 = 1.5*g_0$, $w_1 = 0.9*g_0$ and g_0 = 0.2. (j) Evolution of the dark-field scattering spectra at different polarization directions (0−120°).

In addition, multiple strongly hybridized modes can also result in such broadening effect.[29] The probability of excitation of a plasmonic mode is approximately proportional to the square of its dipole moment. The total dipole moment for a system of n plasmonic particles oscillating in phase is the sum of the individual dipole moments.[12] This collective increase in the dipole moment in this nanosystem leads to enhanced radiative damping rate which thereby can give rise to this super-radiance effect.

The E-field intensity values at the resonant peaks and dips are listed in Table 1. This shows that the average values of enhancement at PII′ and PIII′ (Figure 3) are smaller by a factor of 3.3 and 1.3 (Supporting Information Figure S3) and at DI′ and DII′ higher by a factor of 4.2 and 30.0 compared to their respective values in the SC Dolmen. The smaller values of the field enhancements at the peaks are attributed to the geometry of the structure.[6,38] At DI′ and DII′, the higher enhancement values imply that although this structure is not as efficient in direct excitation of dark modes as the SC system it creates stronger field localization at the Fano dips.

Additional insight into the interactions of the cap NR and the base dimer is revealed by applying the analytical approach as described earlier. Approximate values of resonances of the subunits are obtained from FDTD calculations where; the bright dipolar mode of the cap NR is $\lambda'_{\text{p-cap}}$ = 630 nm and the bright dipolar antibonding mode in the base dimer is $\lambda'_{\text{p-dimer}}$ = 600 nm, the dark bonding mode in the base dimer is $\lambda'_{\text{p-dimer}}$ = 760 nm and a higher order dark mode in the cap is $\lambda'_{\text{d-cap}}$ = 620 nm. The resulting scattering curve (blue) is a linear superposition of the two interactions: (I) $\lambda'_{\text{p-dimer}}$ with $\lambda'_{\text{d-cap}}$ (black curve), and (II) $\lambda'_{\text{p-cap}}$ with $\lambda'_{\text{d-dimer}}$(green curve). Coupling parameters reveal that interaction (B) is weaker than in the SC Dolmen as ($v = 1.5*g_0$ where g_0 = 0.2) and the radiative nature of the dark mode $\lambda'_{\text{d-dimer}}$ ($w = 0.9*g_0$) is significantly lower as compared to the SC Dolmen case (50% narrower peak PIII′, Figure 4h). Geometry of the structure[6] in addition to the lower radiative nature of dark mode and greater spectral overlap between dark and bright modes for interaction (II) are attributed to the stronger E-field localization at the Fano resonance dip DII′ obtained from the FDTD modeled results.

In summary, self-assembled tilted plasmonic Dolmens consisting of substantially smaller NRs of dimensions length ~ 50 nm and diameter ~ 20 nm and small interparticle separations of a few nanometers show plasmonic coherent effects of super-radiance and Fano resonance due to significantly reduced symmetry of the structure. Relative to larger and coarse lithographic nanostructures, the resonances are significantly narrowed by 50%. In addition to the broken symmetry, the strong plasmonic interactions caused by few nanometers gaps enable the observation of multiple radiative and confining plasmonic modes. By tilting the cap monomer with respect to the base dimer an order of magnitude increase of E-field enhancement at the Fano dip is obtained. However, the radiative coupling of the dark mode in the dimer base decreases due to this tilt indicating the strong impact of the geometry of the structure on the nature of coupled modes. Further improvements in E-field localization can be achieved

dx.doi.org/10.1021/nl4007358 | Nano Lett. 2013, 13, 2220−2225

with self-assembly of subunits of different aspect ratios to obtain strongly overlapping dark and bright modes.

The highly localized electric near-fields in few nanometer gaps observed in such structures will enable strong light matter interactions studies including opportunities of enormous spontaneous emission enhancement of fluorophores. Hence these structures have implications in single photon sources, photovoltaic, photodetection, and light emission devices. Moreover the narrow resonances will be useful for improved figure of merits in biomolecule detection. Thus the self-assembled Dolmens with rich optical properties will provide a framework for high quality inexpensive metamaterials for sensing and photonic applications.

■ ASSOCIATED CONTENT

Supporting Information

Further information is provided on the synthesis, modeling, and characterization of the Dolmens. This material is available free of charge via the Internet at http://pubs.acs.org.

■ AUTHOR INFORMATION

Corresponding Author

*E-mail: Richard.Vaia@wpafb.af.mil. Phone: 937-785-9209 Fax number 937- 656-6327.

Notes

The authors declare no competing financial interest.

■ ACKNOWLEDGMENTS

The authors would like to thank K. Park for assistance in synthesis of the base AuNRs, P. Nordlander for insightful comments (MRS Boston, 2012) and V. Giannini and Y. Francescato for assistance in the analytical formulation. Resources for this project were provided by the National Research Council Associateship Program, Materials and Manufacturing Directorate, Air Force Research Laboratory, and the Air Force Office of Scientific Research.

■ REFERENCES

(1) Wu, C.; Khanikaev, A. B.; Adato, R.; Arju, N.; Yanik, A. A.; Altug, H.; Shvets, G. *Nat. Mater.* **2012**, *11*, 69−75.

(2) Hao, F.; Sonnefraud, Y.; Dorpe, P. V.; Maier, S. A.; Halas, N. J.; Nordlander, P. *Nano Lett.* **2008**, *8*, 3983−3988.

(3) Liu, N.; Pucci, A. *Nat. Mater.* **2012**, *11*, 9−10.

(4) Noginov, M. A.; Zhu, G.; Belgrave, A. M.; Bakker, R.; Shalaev, V. M.; Narimanov, E. E.; Stout, S.; Herz, E.; Suteewong, T.; Wiesner, U. *Nature* **2009**, *460*, 1110−1112.

(5) Xu, H.; Aizpurua, J.; Kall, M.; Apell, P. *Phys. Rev. E* **2000**, *62*, 4318−4324.

(6) Wang, J.; Yang, L.; Boriskina, S.; Yan, B.; Reinhard, B. r. M. *Anal. Chem.* **2011**, *83*, 2243−2249.

(7) Pillai, S.; Green, M. A. *Sol. Energy Materials Sol. Cells* **2010**, *94*, 1481−1486.

(8) Fan, P.; Chettiar, U. K.; Cao, L.; Afshinmanesh, F.; Engheta, N.; Brongersma, M. L. *Nat. Photonics* **2012**, *6*, 380−385.

(9) Stockman, M. I. *Opt. Express* **2011**, *19*, 22029−22106.

(10) Schuller, J. A.; Barnard, E. S.; Cai, W.; Jun, Y. C.; White, J. S.; Brongersma, M. L. *Nat. Mater.* **2010**, *9*, 193−204.

(11) Pendry, J. B.; Aubry, A.; Smith, D. R.; Maier, S. A. *Science* **2012**, *337*, 549−552.

(12) Halas, N. J.; Lal, S.; Chang, W.-S.; Link, S.; Nordlander, P. *Chem. Rev.* **2011**, *111*, 3913−3961.

(13) Luo, Y.; Lei, D. Y.; Maier, S. A.; Pendry, J. B. *ACS Nano* **2012**, *6*, 6492−6506.

(14) Liu, M.; Lee, T.-W.; Gray, S. K.; Guyot-Sionnest, P.; Pelton, M. *Phys. Rev. Lett.* **2009**, *102*, 107401.

(15) Solis, D.; Willingham, B.; Nauert, S. L.; Slaughter, L. S.; Olson, J.; Swanglap, P.; Paul, A.; Chang, W.-S.; Link, S. *Nano Lett.* **2012**, *12*, 1349−1353.

(16) Yanik, A. A.; Cetin, A. E.; Huang, M.; Artar, A.; Mousavi, S. H.; Khanikaev, A.; Connor, J. H.; Shvets, G.; Altug, H. *Proc. Natl. Acad. Sci. U.S.A.* **2011**, *108*, 11784−11789.

(17) Giannini, V.; Fernández-Domínguez, A. I.; Sonnefraud, Y.; Roschuk, T.; Fernández-García, R.; Maier, S. A. *Small* **2010**, *6*, 2498−2507.

(18) Luk'yanchuk, B.; Zheludev, N. I.; Maier, S. A.; Halas, N. J.; Nordlander, P.; Giessen, H.; Chong, C. T. *Nat. Mater.* **2010**, *9*, 707−715.

(19) Pena-Rodriguez, O.; Pal, U.; Campoy-Quiles, M.; Rodriguez-Fernandez, L.; Garriga, M.; Alonso, M. I. *J. Phys. Chem. C* **2011**, *115*, 6410−6414.

(20) Shao, L.; Fang, C.; Chen, H.; Man, Y. C.; Wang, J.; Lin, H.-Q. *Nano Lett.* **2012**, *12*, 1424−1430.

(21) Funston, A. M.; Novo, C.; Davis, T. J.; Mulvaney, P. *Nano Lett.* **2009**, *9*, 1651−1658.

(22) Mukherjee, S.; Sobhani, H.; Lassiter, J. B.; Bardhan, R.; Nordlander, P.; Halas, N. J. *Nano Lett.* **2010**, *10*, 2694−2701.

(23) Yang, Z.-J.; Zhang, Z.-S.; Zhang, L.-H.; Li, Q.-Q.; Hao, Z.-H.; Wang, Q.-Q. *Opt. Lett.* **2011**, *36*, 1542−1544.

(24) Woo, K. C.; Shao, L.; Chen, H.; Liang, Y.; Wang, J.; Lin, H.-Q. *ACS Nano* **2011**, *5*, 5976−5986.

(25) Abb, M.; Wang, Y.; Albella, P.; de Groot, C. H.; Aizpurua, J.; Muskens, O. L. *ACS Nano* **2012**, *6*, 6462−6470.

(26) Kern, J.; Großmann, S.; Tarakina, N. V.; Häckel, T.; Emmerling, M.; Kamp, M.; Huang, J.-S.; Biagioni, P.; Prangsma, J. C.; Hecht, B. *Nano Lett.* **2012**, *12*, 5504−5509.

(27) Verellen, N.; Sonnefraud, Y.; Sobhani, H.; Hao, F.; Moshchalkov, V. V.; Dorpe, P. V.; Nordlander, P.; Maier, S. A. *Nano Lett.* **2009**, *9*, 1663−1667.

(28) Zhang, S.; Genov, D. A.; Wang, Y.; Liu, M.; Zhang, X. *Phys. Rev. Lett.* **2008**, *101*, 047401.

(29) Willingham, B.; Brandl, D. W.; Nordlander, P. *Appl. Phys. B: Laser Opt.* **2008**, *93*, 209−216.

(30) Nepal, D.; Park, K.; Vaia, R. A. *Small* **2012**, *8*, 1020.

(31) Slaughter, L. S.; Wu, Y.; Willingham, B. A.; Nordlander, P.; Link, S. *ACS Nano* **2010**, *4*, 4657−4666.

(32) Park, K.; Drummy, L. F.; Wadams, R. C.; Koerner, H.; Nepal, D.; Fabris, L.; Vaia, R. A. *Chem. Mater.* **2013**, *25*, 555−563.

(33) Biswas, S.; Nepal, D.; Park, K.; Vaia, R. A. *J. Phys. Chem. Lett.* **2012**, *3*, 2568−2574.

(34) Giannini, V.; Francescato, Y.; Amrania, H.; Phillips, C. C.; Maier, S. A. *Nano Lett.* **2011**, *11*, 2835−2840.

(35) Oubre, C.; Nordlander, P. *J. Phys. Chem. B* **2005**, *109*, 10042−10051.

(36) Marinica, D. C.; Kazansky, A. K.; Nordlander, P.; Aizpurua, J.; Borisov, A. G. *Nano Lett.* **2012**, *12*, 1333−1339.

(37) Esteban, R.; Borisov, A. G.; Nordlander, P.; Aizpurua, J. *Nat. Commun.* **2012**, *3*, 825.

(38) Mahmoud, M. A.; El-Sayed, M. A. *J. Am. Chem. Soc.* **2010**, *132*, 12704−12710.